New Damage Identification Method for Operational Metro Tunnel Based on Perturbation Theory and Fuzzy Logic

New Damage Identification Method for Operational Metro Tunnel Based on Perturbation Theory and Fuzzy Logic

Ling Wan[a], Xiongyao Xie[b], Lujun Wang[c] *, Pan Li[d], Yong Lu[e]

[a] Lecturer, Dept. of Civil Engineering, College of Engineering, Jiangxi Agricultural University, Nanchang, 330045, China (Email: wanlingstar@126.com)

[b] Professor, Key Laboratory of Geotechnical and Underground Engineering, Ministry of Education, Tongji University, Shanghai, 20092, China (Email: xiexiongyao@tongji.edu.cn)

[c] Associate Professor, Center for Hypergravity Experimental and Interdisciplinary Research, MOE Key Laboratory of Soft Soils and Geoenvironmental Engineering, College of Civil Engineering and Architecture, Zhejiang University, Hangzhou, 310058, China (Email: lujunwang@zju.edu.cn)

[d] Associate Professor, Key Laboratory of Geotechnical and Underground Engineering, Ministry of Education, Tongji University, Shanghai, 20092, China (Email: yongpanli@163.com)

[e] Professor, Institute for Infrastructure and Environment, School of Engineering, The University of Edinburgh, Edinburgh, EH8 9JU, UK (E-mail: E-mail: Yong.Lu@ed.ac.uk)

* CORRESPONDENCE Lujun Wang, lujunwang@zju.edu.cn, Center for Hypergravity Experimental and Interdisciplinary Research, MOE Key Laboratory of Soft Soils and Geoenvironmental Engineering, College of Civil Engineering and Architecture, Zhejiang University, Hangzhou, 310058, China

ABSTRACT

The structural health of operational metro tunnels is closely related to public safety. Prior research has focused on the locations of structural damage, but few researchers have examined both the location of damage and identifying the degree of damage, especially in metro shield tunnels. This paper proposes a new method for identifying structural damage that entails locating and detecting the degradation of tunnel performance, with a special focus on characterizing the degree of damage. First, the dynamic behaviors (modal frequencies and shapes) of different damage levels are obtained from an analytical model of the original tunnel structure. Second, a Modal Strain Energy Damage Indicator (MSEDI) is introduced to locate the damage, regardless of size. Once the location of the damage is identified using MSEDI, a fuzzy logic-based damage identification (FLBDI) method is used to determine the actual extent of the damage. Finally, a simplified model of the tunnel is created using the Euler-Bernoulli beam theory and Winkler's foundation, to further test the procedure under an incomplete modal information condition and with differing noise levels. The results reveal that the fuzzy logic-based system can identify the degree of damage and structural degradation with very high accuracy, in which the location of damage and the prediction of performance degradation is satisfactorily confirmed.

Keywords: metro tunnel; modal strain energy; damage identification; fuzzy logic; dynamic behavior.

1 Introduction

Metro systems have historically played major roles in cities' transportation networks, and the health of metro tunnel structures is crucial for the smooth functioning of the city's transportation systems as well as public safety (Feng *et al.*, 2015).

Due to each tunnel's structural characteristics, different degrees of initial damage exist in normal operational modes. The extent of the damage is affected by both internal and external factors, which also influence each other. Internal factors include the soil medium, ground water, and other environmental considerations (Castaldo *et al.*, 2013 and 2018). External factors include the load of train traffic and construction activities above or nearby the tunnel. In combination, these factors may lead to several problems with the tunnel structure, such as cracks and degradation in the lining, leakage, and cavities. If left unaddressed, significant deformation of the tunnel structure will occur and threaten the stability and safety of the wider tunnel system. Consequently, it may affect the normal operations of the urban rail transit system, and in turn result in further negative social effects (Fu *et al.*, 2019).

In general, exposure to harsh operational and environmental conditions causes metro tunnel structures to gradually deteriorate and require regular maintenance over their service lives (Stajano *et al.,* 2010). Timely detection and identification of damage plays an integral role in the maintenance decisions that ensure the healthy structural conditions of the tunnels. Over the past few decades, monitoring systems have been widely adopted for evaluating the safety and durability of the structures. Structural health monitoring has also been progressively accepted as an effective way to reduce risks for underground structures (Bennett *et al.*, 2010).

Structural health monitoring aims to identify anomalies or damage on a more global basis. The term identification includes the determination of the existence of damage, its location, and the size or degree

of the damage (Anders *et al.*, 1993; Farrar *et al.*, 2007). Many methodologies used for detecting and locating damage have been developed that use modal parameters or their derivatives (Doebling *et al.*, 1996 and 1998). Such methods are established on the premise that the occurrence of structural damage in an engineering system leads to modifications of the vibration modes, i.e., changes in the modal parameters which can be obtained from the results of dynamic (vibration) testing (Salawu *et al.*, 1997).

Most methods rely on descriptions of the damage as an equivalent stiffness reduction at the location of the damage (Gudmundson, 1983; Atluri, 1986; Haisty *et al.*, 1988; Ostachowicz *et al.*, 1991 and Krawczuk, 2002), as a reduction in local stiffness leads to a certain change of dynamic behavior, especially in the modal frequencies. The modal frequency reduction intensifies as the damage grows more severe. Perturbation theory has also been used to describe the dynamic behavior, or curvature modes, of the cracked beams (Luo *et al.*, 1997; Wahyu *et al.*, 2001). Xu et al. (2013) analyzed the characteristics of a multi-damaged plane structure based on local dynamic perturbation. Stepanova et al. (2014) developed an analytical solution to the nonlinear eigenvalue problem that arises from the growth of fatigue cracks in a damaged medium with a coupled formulation. The procedures and algorithms that use modal parameters to back track the structural damage have also been extensively studied.

Xu and Wu (2012) developed an effective damage detection method based on strain data under ambient exaction, and then use it to optimize the installment of strain sensors owing to numerous structural members in the space trusses. Hajrya and Mechbal (2013) established a robust damage detection system based on principal component analysis. Hu et al. (2012) proposed a damage index method for detecting structural damage in cylindrical shells. Li et al. (2013) presented a damage detection method that utilizes changes in eigenvectors with the help of eigenvector perturbation theory. Seyedpoor (2012) proposed a two-step method to identify the site and extent of multiple damage cases in structural systems. First, a

modal strain energy-based index is used to locate the damage. Then, particle swarm optimization (PSO) is used to identify the extent of the damage. Srinivas et al. (2010) demonstrated a multi-stage approach to structural damage identification, using both modal strain energy and evolutionary optimization techniques.

It is generally accepted that vibration-based damage identification methods can be categorized into four levels (Rytter, 1993). The first level is the determination of the presence of damage in the structure. The second level is the determination of the geometric location of the damage. The third level involves quantifying the degree of damage in the structure. The fourth and final level is the residual life assessment of the structure. To date, most of the vibration-based damage identification methodologies can identify only level I and level II damage. When vibration-based methodologies are coupled with structural models, in some cases, level III damage may be identified. In previous research, most vibration-based damage identification methodologies focus on levels I and II of damage detection, and few studies have focused on level III.

This paper presents a new method to describe the global dynamic behavior of a tunnel structure, based on the perturbation theory. The shield tunnel structure is modeled by Euler-Bernoulli beams supported on Winkler foundations. The modal characteristics of the simplified systems are investigated before and after the introduction of tunnel degradation damage. A Modal Strain Energy Damage Indicator (MSEDI) is used to locate the damage, and a fuzzy logic-based damage identification (FLBDI) method is proposed to identity the degree of damage. Among these methods, FLBDI is a well-known approach that can realize the damage identification of level III. Many researchers use FLBDI method applications involving beam structures, and machinery (Ganguli, 2001; Chandrashekhar *et al.*, 2009). This method allows maximum information to be extracted from very limited and uncertain data to roughly identify damaged areas for

1 further nondestructive inspections. The results show that the FLBDI method is capable of realizing level
2 III damage identification for tunnel structures with an accuracy rate of 100%, in which the location of
3 damage and the prediction of performance degradation are satisfactorily determined.
4
5 **2 Tunnel damage analysis based on perturbation theory**
6 **2.1 Tunnel and foundation model**
7 2.1.1 Tunnel model
8 Metro tunnels in soft areas of China are generally constructed using Earth Pressure Balance (EPB)
9 shield machines. The EPB shield is a type of large engineering machinery used in underground space
10 development and shield tunneling. As the EPB shield advances the cutter head rotates to cut the soil into
11 the soil chamber. The passive earth pressure in the soil chamber is balanced with the earth pressure and
12 water pressure on the cutting surface to maintain the stability of the shield excavation surface. The cutter
13 head of the earth pressure shield bears less torque and wear, which is suitable for large diameter and long
14 distance tunnel excavation in soft soil areas.
15 Several researchers have proposed analytical solutions for the bending stiffness of shield tunnels in
16 both the reverse and longitudinal directions, which are the critical parameters for structural design and
17 analysis. In the reverse direction, analytical solutions for estimating the transverse stiffness are based on
18 the equivalence of a jointed shield-driven tunnel lining and a continuous ring structure; the lining is
19 modeled as a rigid pipe without joints, as shown in Fig. 1. In the longitudinal direction, the lining is
20 modeled as is continuously extending along the axis of the tunnel; the lining is represented as a rigid pipe
21 without joints.
22 The bending stiffness coefficient η and convergence deformation can be estimated to analyze the

convergence variations of tunnel rings with different equivalent bending stiffness coefficients. The value corresponding to the stable point is as the equivalent bending stiffness. In this study, the bending stiffness coefficient η was obtained via fine three-dimensional finite element model and model test analysis referred in reference (Wan *et al.*, 2021). The η value is considered to be 0.52.

Previous studies have focused on the bending mode or the flexural deformation of tunnels by treating them as continuous Euler-Bernoulli beams (Zhang *et al.*, 2013). In this paper, the tunnels are also simplified as an Euler-Bernoulli beams, because the main dynamic characteristics are mainly the longitudinal bending mode. The deformation characteristics of Euler-Bernoulli beams are plane sections remaining plane and still being perpendicular to the central axis after deformation. Therefore, the torsional modal and the uncertainty of large shear force are not considered.

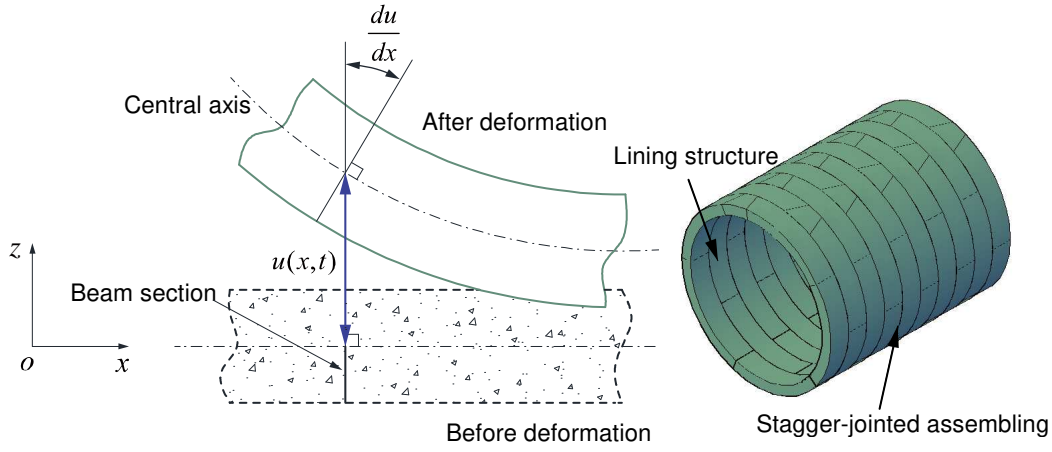

Fig. 1 Deformation characteristics of an Euler-Bernoulli beam

2.1.2 Foundation model

The Winkler foundation model is shown in Fig. 2, and it is used to modelling the interactions between tunnels and the ground (Zhang *et al.*, 2013 and 2015). The Winkler model is a simple foundation model that can give satisfactory results for many practical problems. The hypothesis of the Winkler's foundation posits that the ground is composed of continuously distributed and non-connected discrete springs, where the pressure of a spring is proportional to the ground deflection. This is expressed as:

$$p = ku(x) \tag{1}$$

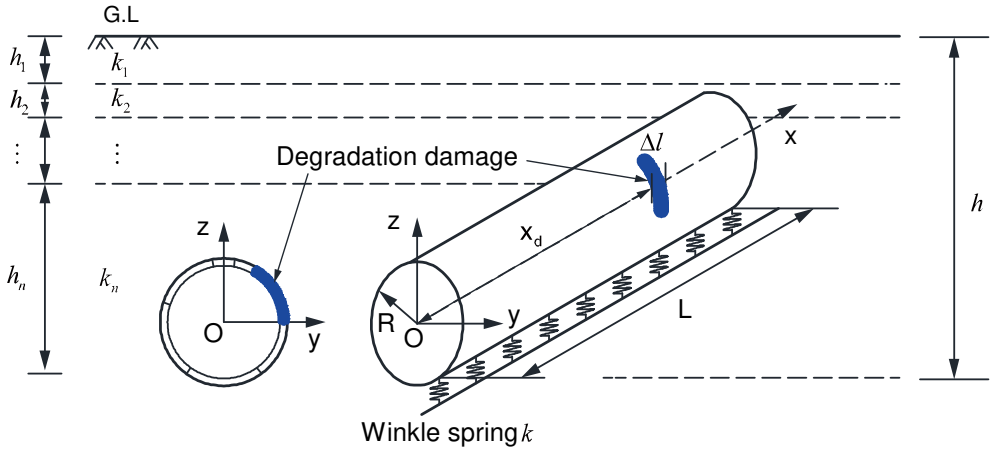

Fig. 2 Winkler foundation model

where p is the pressure applied at the top of the spring; k is the total foundation resistance modulus; and $u(x)$ is the deflection of the ground as well as the neutral axis of the beam.

The total foundation resistance modulus k can be calculated as:

$$k = h/\sum_{i=1}^{n}\frac{h_i}{k_i} \tag{2}$$

where k_i is the foundation resistance modulus of each soil layer, h_i is the thicknesses of the i^{th} layer, and h is the thickness of compressible stratum.

The Winkler model is a simple foundation model and can give satisfactory results for metro tunnel problems (Liang *et al.*, 2017; Yu *et al.*, 2014). As the torsional contact effect is much smaller than that of the vertical foundation contact, the uncertainty caused by torsional contact between soil and tunnel is negligible. In this paper, the Winkler foundation model is used to model the tunnel ground interaction.

2.1.3 Tunnel degradation damage

As shown in Fig. 2, the tunnel degradation damage is allocated along the longitudinal direction. The bending stiffness of the damaged tunnel can be described along the longitudinal direction as:

$$EI(x) = EI^{eq}[1 - \beta(H(x - x_d) - H(x - x_d - \Delta l)] \tag{3}$$

where β is the degradation degree, x_d is the damage coordinate along the longitudinal direction, and

Δl is the damage width. $H(x)$ is the Heaviside step function and is defined as:

$$H(x) = \begin{cases} 1 & x \geq 0 \\ 0 & x < 0 \end{cases} \tag{4}$$

Thus, the bending stiffness of the damaged cross section is βEI^{eq}, ranging from x_d to $x_d + \triangle l$, and the bending stiffness of the undamaged cross section is $(EI)^{eq}$. Therefore, Eq. (2) can be rewritten as:

$$EI(x) = EI^{eq}(1 - \beta \triangle l\delta(x - x_d)) \tag{5}$$

where $\delta(x) = \frac{dH(x)}{dx}$ represents the Dirac delta function.

2.2 Derivation of an analytical solution

A two-stage analysis method is utilized in this section, including structural modal analysis and dynamic response analysis, is utilized in this section. The degradation of the tunnel degradation damage is divided into two stages: first, perturbation theory is introduced to establish the characteristic equation of the damaged tunnel structure, based on the hypothesis that the change of structural dynamic characteristics relates to the damage degree of damage. Second, Fourier series are used to solve the established characteristic equations.

The tunnel is simplified as an Euler-Bernoulli beams resting on a Winkler foundation. The equilibrium equations of the longitudinal motion are derived and are solved by Fourier series based on perturbation theory.

2.2.1 Perturbation solution

To acquire the governing equations of beam equilibrium, an element is selected to perform the force analysis, as shown in Fig. 3.

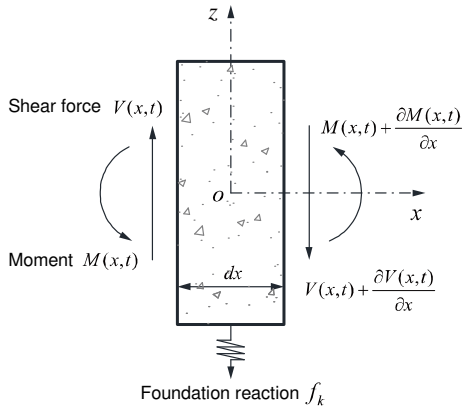

Fig. 3 Force analysis of an element

The motion equation in the z direction can be expressed as:

$$V(x,t) + f_k - \left(V(x,t) + \frac{\partial V(x,t)}{\partial x}dx\right) - f_I = 0 \tag{6}$$

where $V(x,t)$ is shear force. f_k is the foundation resistance force, $f_k = ku(x,t)dx$, f_I is the inertia force, $f_I = m\frac{\partial^2 u(x,t)}{\partial^2 t}$. Substituting f_k and f_I into Eq. (6), one obtains:

$$\frac{\partial V(x,t)}{\partial x} = f_k - m\frac{\partial^2 u(x,t)}{\partial t^2} \tag{7}$$

The bending moment equilibrium about the right end of the segment yields:

$$M(x,t) + V(x,t)dx - (M(x,t) + \frac{\partial M(x,t)}{\partial x}dx) = 0 \tag{8}$$

where $M(x,t)$ is the moment. Rearranging Eq. (8) gives:

$$\frac{\partial M(x,t)}{\partial x} = V(x,t) \tag{9}$$

Substituting Eq. (9) into Eq. (7) gives:

$$\frac{\partial^2 M(x,t)}{\partial x^2} + \overline{m}\frac{\partial^2 u(x,t)}{\partial t^2} = f_k \tag{10}$$

The relationship between bending moment and curvature in the longitudinal direction gives:

$$M(x,t) = EI\frac{\partial^2 u(x,t)}{\partial x^2} \tag{11}$$

Substituting Eq. (11) into Eq. (10) gives:

$$\frac{\partial^2}{\partial x^2}(EI\frac{\partial^2 u(x,t)}{\partial x^2}) + \overline{m}\frac{\partial^2 u(x,t)}{\partial t^2} = f_k \tag{12}$$

The solution for Eq. (12) can be obtained through the variable separation method.

$$u(x,t) = \phi(x)e^{-i\omega t} \tag{13}$$

where $\phi(x)$ and ω are respectively eigenvector and circular frequency. Substituting Eq. (13) into Eq. (12) gives:

$$\frac{\partial^2}{\partial x^2}\left(EI^{eq}(1-\beta \triangle lc)\frac{\partial^2\phi_i(x)}{\partial x^2}\right) - (\overline{m}\lambda_i + K)\phi_i(x) = 0 \tag{14}$$

where $\lambda = \omega^2$ is the eigenvalue. Subscript i represents the modal order. The eigenvalue and eigenvector solutions for the damaged tunnel structure can be expressed as perturbations of the changes between the damaged and undamaged tunnel, so the eigenvalue and eigenvector can respectively be expressed as (Chen, 2007):

$$\lambda_i = \lambda_i^0 - \beta\lambda_i^1 \tag{15a}$$

$$\phi_i = \phi_i^0 - \beta\phi_i^1 \tag{15b}$$

where λ_i^0 and ϕ_i^0 are the eigenvalue and eigenvector solutions for the undamaged tunnel, while λ_i^1 and ϕ_i^1 are the first order perturbation of the eigenvalue and eigenvector for the damaged tunnel. Substituting Eq. (15a) and Eq. (15b) into Eq. (14), and collecting the same exponentiation coefficient of β, one obtains:

$$\beta^0: \quad EI^{eq}\frac{\partial^4\phi_i^0}{\partial x^4} - \overline{m}\lambda_i^0\phi_i^0 - k\phi_i^0 = 0 \tag{16a}$$

$$\beta^1: \quad EI^{eq}\frac{\partial^4\phi_i^1}{\partial x^4} + \beta \triangle lEI^{eq}\frac{\partial^2}{\partial x^2}(\delta(x-x_d)\frac{\partial^2\phi_i^0}{\partial x^2}) - \overline{m}\lambda_i^0\phi_i^1 - k\phi_i^0 = 0 \tag{16b}$$

2.2.2 Solution of perturbation equations using Fourier series

The i^{th} order eigenvector and eigenvalue of the elastic foundation tunnels can respectively be given by (Beena *et al.*, 2011):

$$\lambda_i^0 = (\frac{i\pi}{L})^4\frac{EI^{eq}}{\overline{m}} + \frac{k}{\overline{m}} \tag{17a}$$

$$\phi_i^0 = sin\frac{i\pi x}{L} \tag{17b}$$

The first order perturbation of i^{th} modal shape ϕ_i^1 is given by (Chandrashekhar *et al.*, 2009):

$$\phi_i^1 = \sum_{k=1}^{N} a_{ik}\phi_k^0 \tag{18}$$

An approximate solution for Eq. (18) can be obtained by imposing a solution that corresponds to the Fourier series expansion of the perturbation mode:

$$\phi_i^1 = \sum_{k=1}^{N} a_{ik} sin\frac{i\pi x}{L} \tag{19}$$

Substituting this Fourier series expansion into Eq. (16b) gives:

$$\begin{gathered} EI^{eq}\sum_{k=1}^{N} a_{ik}\left(\frac{i\pi}{L}\right)^4 sin\frac{i\pi x}{L} - \beta\ \ EI^{eq}\Delta l\frac{\partial^2}{\partial x^2}(\delta(x-x_d)(\frac{i\pi}{L})^2 sin\frac{i\pi x}{L}) \\ -m\lambda_i^0\sum_{k=1}^{N} a_{ik}\, sin\frac{i\pi x}{L} - \lambda_i^1 sin\frac{i\pi x}{L} - k\sum_{k=1}^{N} a_{ik} sin\frac{i\pi x}{L} = 0 \end{gathered} \tag{20}$$

Eq. (20) is multiplied by $sin\frac{j\pi x}{L}$, then distributing the integral over the whole length of the elastic foundation beam. The complexity can be substantially reduced by exploiting the orthogonality properties of harmonic functions, giving:

$$\int_0^L \left\{ \begin{gathered} EI^{eq}\sum_{k=1}^{N} a_{ik}\left(\frac{i\pi}{L}\right)^4 sin\frac{i\pi x}{L} - \beta\ \ EI^{eq}\Delta l\frac{\partial^2}{\partial x^2}(\delta(x-x_d)(\frac{i\pi}{L})^2 sin\frac{i\pi x}{L}) \\ -m\lambda_i^0\sum_{k=1}^{N} a_{ik}\, sin\frac{i\pi x}{L} - \lambda_i^1 sin\frac{i\pi x}{L} - k\sum_{k=1}^{N} a_{ik} sin\frac{i\pi x}{L} \end{gathered} \right\} sin\frac{j\pi x}{L}dx = 0 \tag{21}$$

Eq. (21) can be simplified by taking advantage of the delta function (Kosko, 1997):

$$f(x)\delta(x-x_0) = f(x_0)\delta(x-x_0) \tag{22}$$

$$\int_{-\infty}^{+\infty} f(x)\,\delta(x-x_0)dx = f(x_0) \tag{23}$$

Eq. (21) can be simplified as:

$$EI^{eq}\frac{L}{2}\left(\frac{\pi}{L}\right)^4 (j^4 - i^4)a_{ij} + \beta\ \ EI^{eq}\Delta l i^2(\frac{\pi}{L})^2 sin\frac{i\pi x_d}{L} sin\frac{j\pi x_d}{L} - \lambda_i^1\frac{L}{2}\delta_{ij} - ka_{ij}\frac{L}{2} = 0 \tag{24}$$

The amplitude of the Fourier series coefficients a_{ij} can be obtained by letting $i \neq$ j in Eq. (24):

$$a_{ij} = \frac{2\beta\Delta l i^2 j^2}{L(\frac{kL^4}{\pi^4 EI} + i^4 - j^4)}\ \ sin\frac{i\pi x_d}{L} sin\frac{j\pi x_d}{L} \tag{25}$$

The amplitude of the Fourier series coefficients a_{ii} can be obtained according to the condition of orthogonality:

$$\int_0^L \phi_i \overline{m}\phi_i = 1 \tag{26}$$

Substituting Eq. (15b) into Eq. (26) gives:

$$a_{ii} = \beta/2 \tag{27}$$

Substituting Eq. (27) into Eq. (24) gives:

$$\lambda_i^1 = 2EI\frac{\Delta l}{L}(\frac{i\pi}{L})^4 sin^2\frac{i\pi x_d}{L} - \frac{k\beta}{2} \tag{28}$$

The above formulations are used to assess the influence of the degree and the location of damage on the foundation beam tunnel. The modal frequencies (or eigenvalues) and modal shapes (or eigenvectors) can be computed from the obtained perturbation solutions and are given by:

$$\lambda_i = \lambda_i^0 - 2\beta EI\frac{\Delta l}{L}\left(\frac{i\pi}{L}\right)^4 sin^2\frac{i\pi x_d}{L} + \frac{k\beta^2}{2} \tag{29a}$$

$$\phi_i = \phi_i^0 - \beta(\sum_{\substack{i=1 \\ i\neq j}}^{N} a_{ij}\,\phi_j^1 + a_{ii}\phi_i^1) \tag{29b}$$

2.3 Tunnel damage location identification using MSEDI

Modal shape variations are different in differing damage elements, and the modal shape variations contain the information about the location of damage. To locate and identify the structural damages, MSEDI is employed. The flowchart of the procedure is shown in Fig. 4.

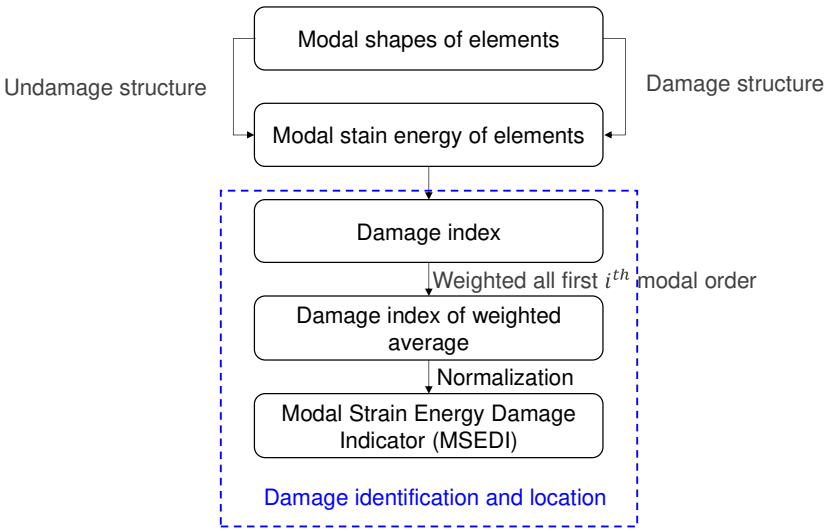

Fig. 4 Flowchart of damage identification using MSEDI

The concept of Modal Strain Energy (MSE) was firstly proposed and the applied to the beam (Chen *et*

al., 1998). Mode shapes can be utilized for evaluating the MSE of tunnel structure. The i^{th} order MSE for a thin-wall circular shell beam can be expressed as:

$$MSE_i = \frac{1}{2}\phi_i^T EI\phi_i \tag{30}$$

Dividing the thin-wall circular shell beam into k elements along the longitudinal direction, the i^{th} MSE of the k^{th} element can be expressed as:

$$MSE_{i,k}^0 = \frac{1}{2}(\phi_{i,k}^0)^T EI_k\phi_{i,k}^0 \tag{31a}$$

$$MSE_{i,k}^d = \frac{1}{2}(\phi_{i,k}^d)^T EI_k\phi_{i,k}^d \tag{31b}$$

where $MSE_{i,k}^0$ and $MSE_{i,k}^d$ denote the i^{th} MSE of the k^{th} element for the undamaged and damaged structure, respectively. Thus, the change of the MSE after damage can be written as:

$$\vartheta_{i,k} = \left|MSE_{i,k}^0 - MSE_{i,k}^d\right| \tag{32}$$

where $\vartheta_{i,k}$ represents the i^{th} modal order variations of MSE of k^{th} element after damage. Considering all measured modal orders and taking $\vartheta_{i,k}$ to normalize and get MSEDI, the k^{th} element it gives:

$$\text{MSEDI} = \vartheta_k / \sum_{i=1}^{k}\vartheta_{i,k} \tag{33}$$

where the MSEDI represents the mean damage indicator for the k^{th} element and is used to predict the location of damage in the foundation beam that represents the tunnel structure. The MSEDI is a dimensionless indicator that ranges from 0 to 1.

2.4 Tunnel damage degree identification based on FLBDI

2.4.1 Fuzzy logic systems

Fuzzy logic systems (FLS) are computational mechanisms based on fuzzy sets, fuzzy rule and fuzzy inferences. FLSs can also perform the nonlinear mapping between inputs and outputs (Zedeh, 1996;

Pawar *et al.*, 2007; Srinivas *et al.*, 2011; Zhao *et al.*, 2002 and Reda Taha *et al.*, 2005). Fuzzy set theory and fuzzy logic provide the framework for the non-linear mapping.

Nonlinear mapping using FLS involves turning an input feature vector into a scalar output. A typical multi-input single-output (MISO) that FLS performs is mapping from $x \in R^m$ to $y \in V$, as follows:

$$f:\ x \in R^m \rightarrow y \in V \tag{34}$$

where $x = (x_1, x_2, \ldots \ldots x_m) \in R^m$ is the input space and $y \in V$ is the output space.

The Mamdani fuzzy system is a widely used mapping system which consists of four basic components: the fuzzier of input data, the fuzzy rule base, fuzzy inference, and the de-fuzzier of output data, as shown in Fig. 5.

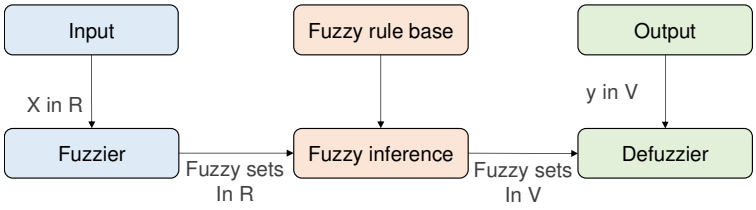

Fig. 5 Schematic representation of Mamdani fuzzy systems

The fuzzy rules can be obtained either from experts or numerical data. Rules are expressed as a collection of IF-THEN statements such as 'IF x_1 is HIGH, and x_2 is LOW, THEN y is HIGH'. Based on FLS, FLBDI is used for the identification of the degree of damage to the elastic foundation beam that represents the tunnel structure. Combined with the location of damage presented in the previous sections, this procedure will enable the identification of level III damage. A schematic representation of the tunnel structure based on FLBDI is shown in Fig. 6.

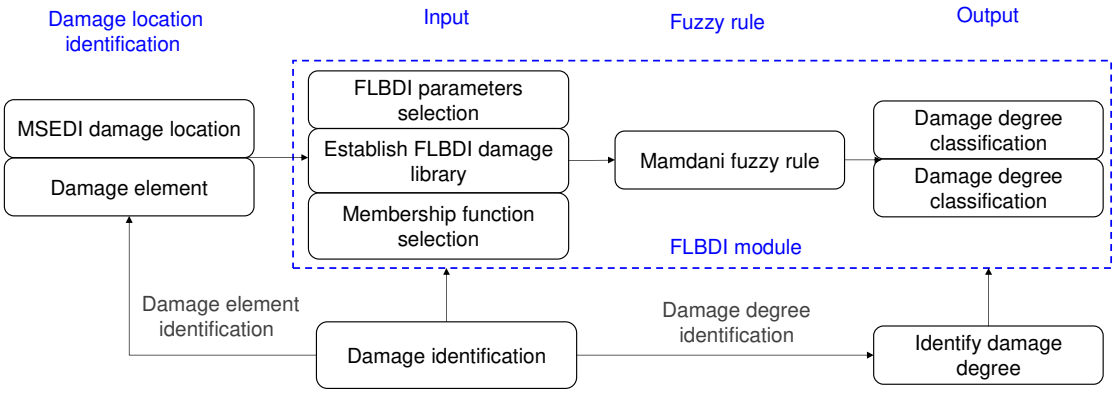

Fig. 6 Schematic representation of tunnel structure based on FLBDI

2.4.2 Tunnel damage degree identification with incomplete information

The inputs to the FLBDI contain the modal information of structure nodes, such as modal shape amplitudes, or other variants decided by considering the actual situation of the structural damage. Outputs are the parameters of the degree of structural damage.

It is unnecessary and impractical that data at all nodes are obtained or measured in an actual application, considering the generally limited number of sensors used and other practical factors. How to realize the the best identification of the degree of damage with incomplete information is important.

The follow the flow of FLBDI method, used to identify the damage to tunnel under incomplete information, is as follows.

(1) Input

A complete set of information would include the modal shape variation data at all nodes. Suppose that the set of available information consists of only some incomplete nodes, whereas the remaining nodes are unmeasured, including lost or invalid measurements. The input vectors may be expressed as follows:

$$\mathrm{R} = \{\Delta\phi_i, \Delta\phi_j, \ldots, \Delta\phi_n\} \tag{35}$$

The modal shape variations at node i to n are selected as the FLBDI module inputs, and the membership functions of the inputs are assumed to follow the rules of Gaussian function. The input data,

which can be well controlled through adjusting the control parameters of the Gaussian function, also reflect can be well reflected the fuzzy characteristic of the FLBDI module. The FLBDI module inputs, then, are written as:

$$\mu(x) = e^{-(\frac{x-a}{b})^2}, b > 0 \tag{36}$$

where [a, b] are the control parameters of the membership function. These control parameters are decided by considering the actual type of damage to the structure.

(1) Output

In this paper, the damage degrees are classified into four states, including undamage, slight, moderate and severe damage. The damage degree is determined by the damaged area of tunnel segments and the degradation degree β. If there is a small damaged area with very small degradation degree β, it can be classified as undamaged (where damage degree is about 1%-5%). If there is a small damaged area with small degradation degree β, it can be classified as slight (the damage degree of about 5%-15%). If there is a moderate damaged area with small or moderate degradation degree β, it can be classified as moderate (15%-30%). If there is a large damaged area with moderate or severe degradation degree β, it can be classified as severe (over 30%), as shown in Table 1. The membership functions for the four damage states are defined in Eq. (37).

Table 1 Damage degree classifications

Degree	Undamage	Slight	Moderate	Severe
Degradation	0%-5%	5%-15%	15%-30%	≥30%

$$\mu(y) = \frac{1}{1+\left|\frac{y-c}{a}\right|^{2b}} \tag{37}$$

where [a,b,c] are the control parameters of the membership function.

3 Tunnel damage location identification

To validate the feasibility and sensitivity of the proposed damage identification approach, a metro tunnel structure in Shanghai Metro Line 12 is used in this study. The tunnel lining is C50 reinforced concrete. The material properties are shown in Table 2.

Table 2 Material properties for the sample tunnel structure

Length (m)	External radius (m)	Internal radius (m)	Buried depth (m)	Thickness (m)	Density (kg/m3)	Elastic modulus (MPa)
80	3.1	2.75	28.2	0.35	2450	34500

The soil stratums and its foundation resistance coefficient values are shown in Table 3, the values are based on the geotechnical investigation and engineering experience values of Shanghai stratums.

Table 3 Parameters for the stratums

Stratum	Thickness (m)	Foundation resistance coefficient (kN/m^3)
①$_2$ Silt	3	2280
⑤$_{1\text{-}1}$ Mud	2.7	2670
⑤$_{1\text{-}2}$ Silty clay	2.8	3780
⑥ Clay	4.7	6010
⑦$_1$ Sand silt	7.8	11780
⑦$_2$ Sand	7.2	12780

The length of the elastic foundation beam model is 80 m. The model consists of 9 nodes and 8 elements, as shown in Fig. 7. The bending rigidity is EI=9.5272x10^8 kN·m^2, and the total foundation resistance coefficient is k=5556.3 kN/m^3.

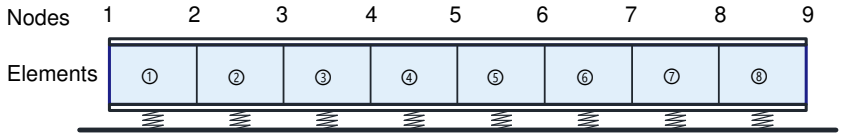

Fig. 7 Elastic foundation beam model

3.1 Scenario type A: Different damage elements

Assuming a 10% degradation of rigidity at elements ②, ④ and ⑥, respectively, the modal characteristics of the elastic foundation beam are analyzed. The modal frequencies are shown in Table 4.

Table 4 Modal frequencies

Modal order	Undamaged (Hz)	Damaged element (Hz)

		element ②	element ④	element ⑥
1	1.766	1.765	1.761	1.761
2	4.083	4.064	4.063	4.063
3	8.682	8.601	8.669	8.668
4	15.279	15.108	15.109	15.108
5	23.807	23.579	23.768	23.768

The modal frequency variations with differing damage elements vary, and those variations are very small for the 10% degradation in an individual element, with the maximum variation ratio being 1.12%. Therefore, the modal frequencies are not sensitive to degradation.

Table 5 Maximum frequency variation ratios with different damage elements

Modal order	1st order	2nd order	3rd order	4th order	5th order
Maximum frequency variation ratios	0.28%	0.49%	0.93%	1.12%	0.96%

The identification results for the three damage scenarios are given in the following subsections, as shown in Fig. 8.

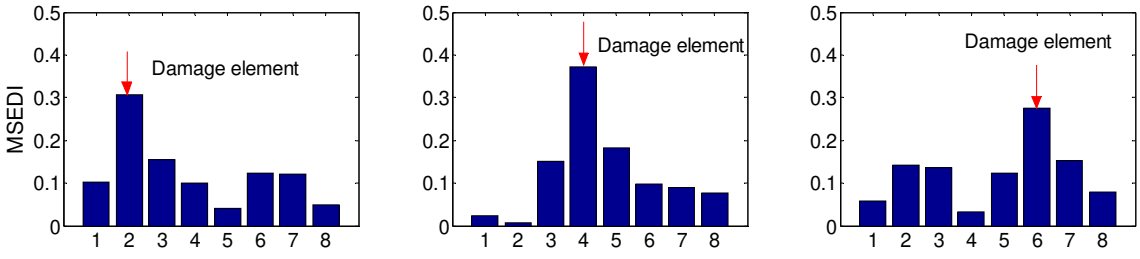

(a) Element ② (b) Element ④ (c) Element ⑥

Fig. 8 MSEDI results with different damage elements with 10% degradation

There are three clear peaks at the location of element ② in Fig. 6 (a) , element ④ in Fig. 6 (b) and element ⑥ in Fig. 6 (c), which corresponds to the actual damage locations. As a result, it correctly identifies the actual location of the damage to the tunnel structure.

3.2 Scenario type B: Different damage degrees

For this scenario, the damage is fixed at element ②, but the degrees vary from 10% , to 20%, to 30% degradation and are analyzed using the modal characteristics of the elastic foundation beam. The modal frequencies are shown in Table 6.

Table 6 Modal frequencies

Modal order	Undamaged	Degradation of damage element ②		
		10%	20%	30%
1	1.766	1.765	1.764	1.763
2	4.083	4.063	4.047	4.035
3	8.682	8.601	8.537	8.492
4	15.279	15.108	14.974	14.877
5	23.807	23.579	23.399	23.271

The modal frequency variations with differing degrees are also distinct, and in general the more degradation, the greater the variations, with the maximum variation ratio being 2.63%. As a result, the modal frequencies are not so sensitive to degradation.

Table 7 Maximum frequency variation ratios with different damage elements

Modal frequency variation ratio	1st order	2nd order	3rd order	4th order	5th order
10% degradation	0.05%	0.49%	0.93%	1.12%	0.96%
20% degradation	0.09%	0.9%	1.67%	1.99%	1.71%
30% degradation	0.11%	1.15%	2.19%	2.63%	2.26%

To identify and locate the damage, a reproduction parameterization based on modal shape parameter is utilized. The flowchart of damage identification is shown in Fig. 4.

The location of the damage in the damage element with 10%, 20%, and 30% degradation is identified through the evolution analysis of the modal shapes that resulted from that element. The results are shown in Fig. 9.

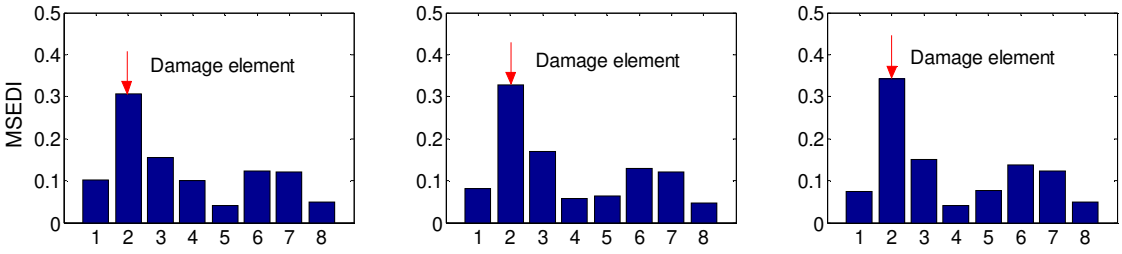

(a) 10% degradation (b) 20% degradation (c) 30% degradation

Fig. 9 Damage location with different degradation of element ②

There are three clear peaks at the location of element ② in Fig. 7. The element ② features degradation damages, which are corresponding to the actual locations of the damage. So, the indicator

correctly identifies the actual location of the damage.

The above analysis shows that MSEDI can be used to effectively identify the location of the damage, even when the degree of the damage is small, and the MSEDI will be considered to tunnel model experiments to study the damage location of tunnel lining degradation in the future. However, the absolute values of MSEDI have no direct relation to the severity of the damage, so MSEDI may only be used for locating the damage and additional techniques are required to further assess the damage degree of the damage. This will be discussed in the next section.

4 Tunnel damage degree identification with incomplete information

4.1 FLBDI parameters and fuzzy rules

Recall the perturbation solution from the modal analysis for a damaged section of a tunnel as discussed previously, taking the damage element ④ with 2%, 10% and 22% degradations as an example. The mode shape variations at node 2 to 5 ($R = \{\Delta\phi_2, \Delta\phi_3, \Delta\phi_4, \Delta\phi_5\}$) are selected as the FLBDI module inputs. For the analysis examples herein, each set of input node values are classified into four levels, VL (very low), L (low), M (Middle), H (high). And the FLBDI input membership of each node is shown in Fig. 10. The membership function parameters are given in Table 8.

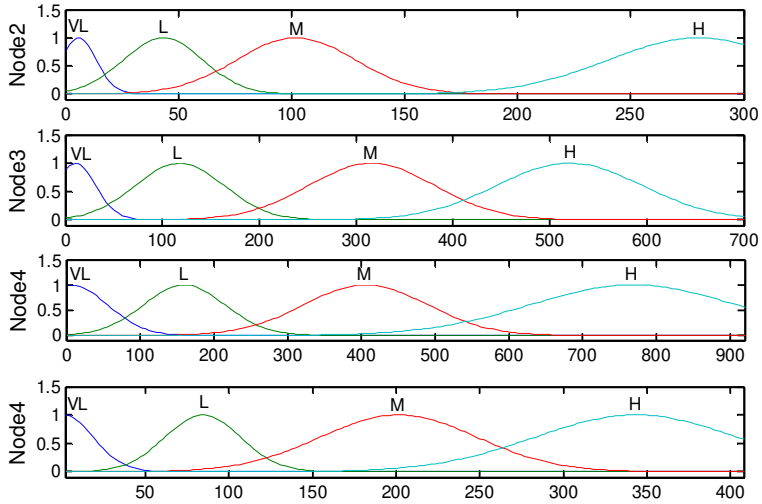

Fig. 10 Inputs membership of each node

Table 8 Membership function parameters

Damage degree	Parameter a	Parameter b	Parameter c
Undamage	3	2.5	0
Slight	5	2.5	10
Moderate	5	2.5	22.5
Severe	3	2.5	30

To determine the appropriate control parameters of the input membership function for the analysis case with damage at element 4, the FLBDI damage library for the element needs to be established. Firstly, we need to analyze the input values relating to several typical degrees of damage. So, for element 4, we select a) the undamaged state (up to 3% degradation), b) slight damage (12% degradation), c) moderate damage (20% degradation), and severe damage (35% degradation). The mode shape variations of node 2 to 5 are shown in Table 9.

Table 9 FLBDI damage library of damage element ④

Typical damage	$\Delta\phi_2$ (10^{-7}m)	$\Delta\phi_3$ (10^{-7}m)	$\Delta\phi_4$ (10^{-7}m)	$\Delta\phi_5$ (10^{-7}m)
Undamage (3%)	2.08	5.14	6.74	2.99
Slight (12%)	33.3	82.2	108	47.8
Moderate (20%)	92.5	228	300	133
Severe (35%)	283	699	918	407

The Mamdani system's fuzzy rules are adopted, as shown in Table 10, and the FLBDI module of the damaged tunnel with incomplete information is shown in Fig. 11.

Table 10 Fuzzy rules of damage tunnel

Output	Inputs			
	Node2	Node3	Node4	Node5
Undamage	VL	VL	VL	VL
Slight	L	L	L	L
Moderate	M	M	M	M
Severe	H	H	H	H

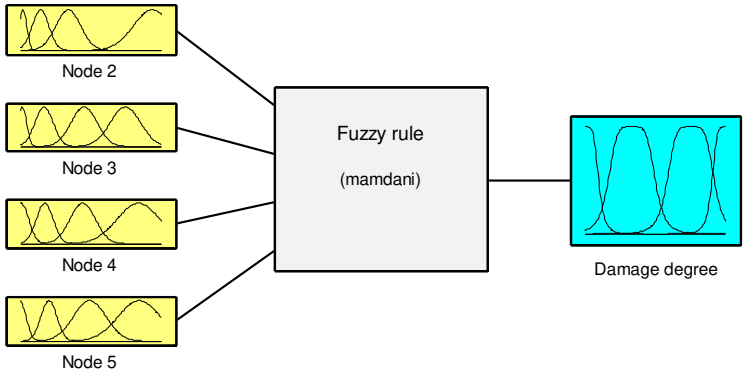

Fig. 11 FLBDI module of damage tunnel under incomplete information

4.2 Tunnel damage degree identification results

4.2.1 Damage element ④ with 2% degradation

The input data for node 2 to 5 are 0.96, 2.28, 2.99 and 1.33, respectively. Through the FLBDI module, the damage identification results are shown in Fig. 12. The output is a degree of damage of 2.01%, which belongs to the undamaged state. This corresponds with the actual damage of 2%.

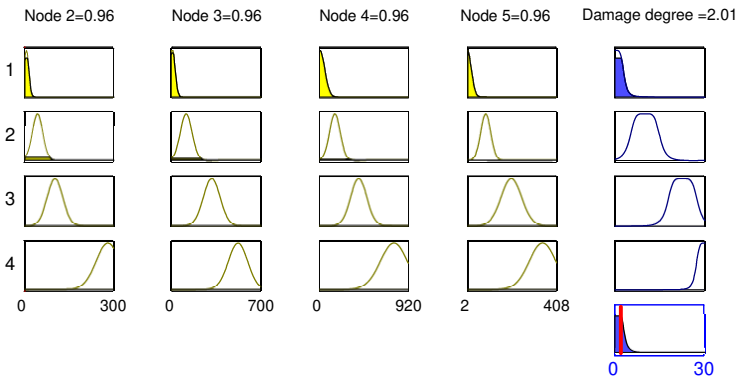

Fig. 12 FLBDI result of element ④ with 2% degradation

4.2.2 Damage element ④ with 10% degradation

The input data of nodes 2 to 5 are 23.13, 57.09, 74.94 and 33.22, respectively. Through the FLBDI module, the damage identification results are shown in Fig. 13. The output is a 10% degree of damage, which belongs to the slight damage state. This also corresponds to the actual degree of damage of 10%.

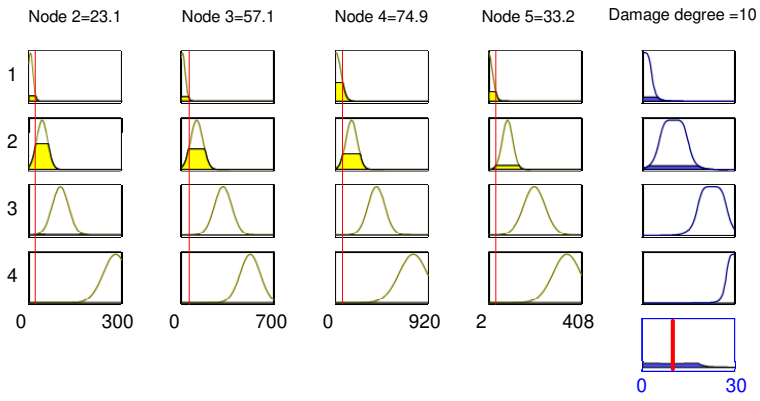

Fig. 13 FLBDI result of element ④ with 10% degradation

4.2.3 Damage element ④ with 22% degradation

The input data in this case for nodes 2 to 5 is 144.55, 365.85, 468.35 and 207.65, respectively. Through the FLBDI module, the damage identification results are shown in Fig. 14. The output is a 22% degree of damage, which belongs to the moderate damage state. This matches with the actual degree of damage of 22%.

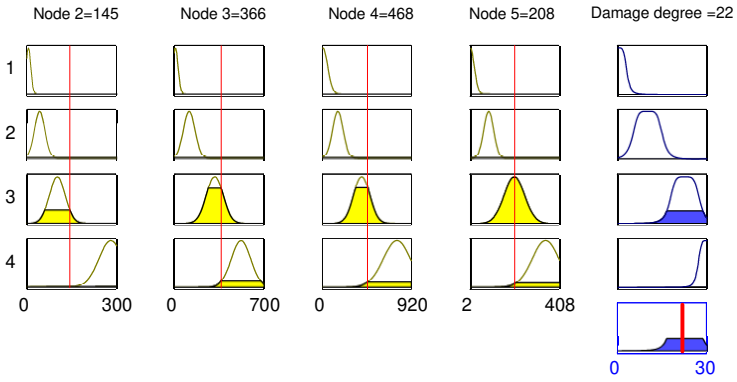

Fig. 14 FLBDI result of element ④ with 22% degradation

The uncertain node information selection affects the identification results. The identification accuracy is more than 99% under incomplete node information conditions.

4.3 Tunnel damage degree identification under different noise levels

The FLBDI module is tested using noise contaminated information data at the input nodes. The noise in the input parameters is simulated herein by adding white Gaussian white noise (Chandrashekhar *et al.*,

2009), and is expressed as follows:

$$r_{noise} = r_{i,n}(1 + \lambda normrnd(0,1)) \tag{38}$$

where r_{noise} denotes a parameter value with noise, $r_{i,n}$ denotes the parameter without noise, λ is the noise level parameter, and $normrnd(0,1)$ is the Gaussian random number.

Three new sets of examples are given below.

4.3.1 Damage element ④ with 2% degradation

The noise levels are respectively selected are 5%, 10%, 15% and 20% to demonstrate the noise-resistance ability of the FLBDI based method. The noise-contaminated input data under different noise levels is listed in Table.11. Through the FLBDI module, the damage identification results are shown in Fig. 15.

Table.11 Inputs data of FLBDI under different noise levels

Noise level	Inputs			
	Node2	Node3	Node4	Node5
Non-noise	0.96	2.28	2.99	1.33
$\lambda = 5\%$	0.97	2.32	3.03	1.35
$\lambda = 10\%$	0.99	2.35	3.08	1.37
$\lambda = 15\%$	1.01	2.39	3.13	1.39
$\lambda = 20\%$	1.02	2.43	3.18	1.41

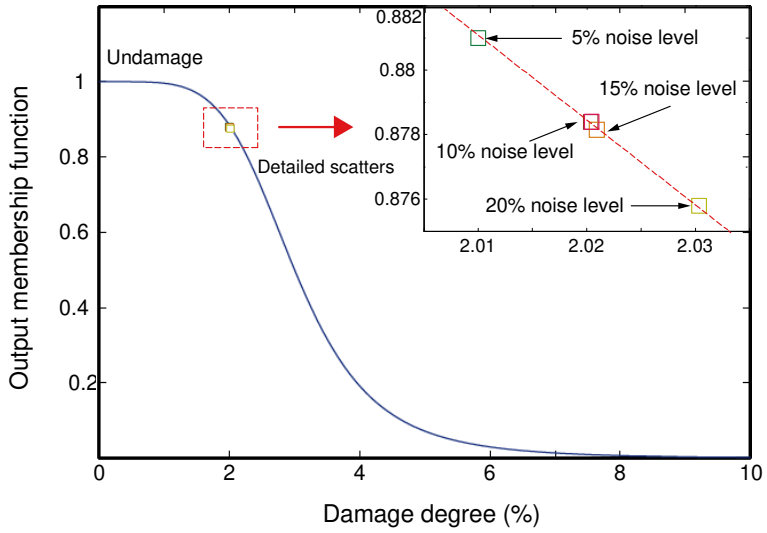

Fig. 15 FLBDI results of element ④ with 2% degradation under different noise levels

Figure 15 shows the identification of the degree of damage as 2.01%, 2.02%, 2.02% and 2.03% under

the noise levels of 5%, 10%, 15% and 20%. The outputs all fit to the undamaged state, and this corresponds with the actual degree of damage. The results suggest that the FLBDI method has excellent noise resistance, and in the example it can accurately identify the tunnel degree of damage to the tunnel under a 20% noise level.

4.3.2 Damage element ④ with 10% degradation

The noise level parameters respectively selected are 5%, 10%, 15% and 20%. The noise-contaminated input data under different noise levels can be seen in Table.12. Using FLBDI module, the damage identification result can be seen in Fig. 16.

Table.12 Inputs data of FLBDI under different noise levels

Noise level	Inputs			
	Node2	Node3	Node4	Node5
Non-noise	23.13	57.09	74.94	33.22
$\lambda = 5\%$	23.49	57.99	76.13	33.75
$\lambda = 10\%$	23.87	58.91	77.33	34.28
$\lambda = 15\%$	24.24	59.82	78.52	34.81
$\lambda = 20\%$	24.61	60.73	79.72	35.34

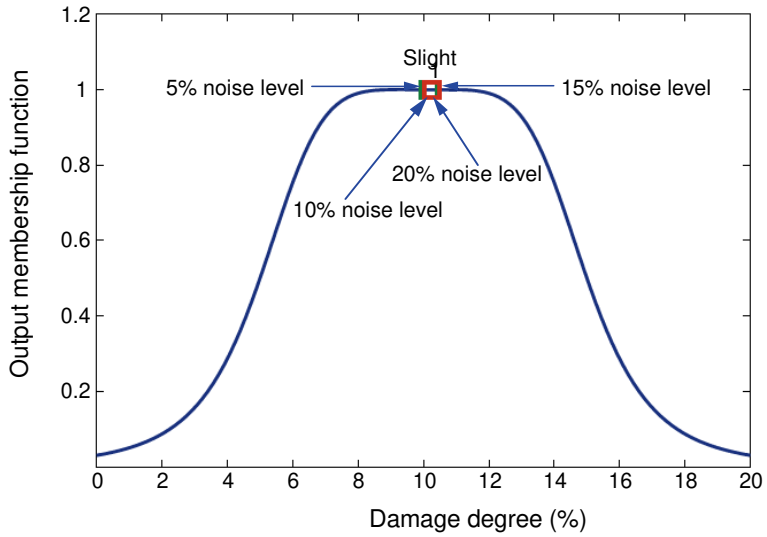

Fig. 16 FLBDI results of element ④ with 10% degradation under different noise levels

As seen in figure 16, the results of the identification of the degree of damage are 10.2%, 10.2%, 10.3% and 10.3%, under the noise levels of 5%, 10%, 15% and 20%. The outputs can all be classified as 'Slight', which corresponds to the actual degree of damage. Accordingly, the FLBDI method has excellent

character of anti-noise characteristics and can accurately identify the degree of damage to a tunnel under a noise level of 20%.

4.3.3 Damage element ④ with 22% degradation

The noise level parameters selected for this example are 5%, 10%, 15% and 20%. The noise-contaminated input data under the different noise levels can be seen in Table.13. Using the FLBDI module, the damage identification result can be seen in Fig. 17.

Table.13 Inputs data of FLBDI under different noise levels

Noise level	Inputs			
	Node2	Node3	Node4	Node5
Non-noise	144.55	365.85	468.35	207.65
$\lambda = 5\%$	146.85	371.67	475.77	210.95
$\lambda = 10\%$	149.16	377.52	483.29	214.27
$\lambda = 15\%$	151.46	383.34	490.74	217.57
$\lambda = 20\%$	153.77	389.19	498.23	220.89

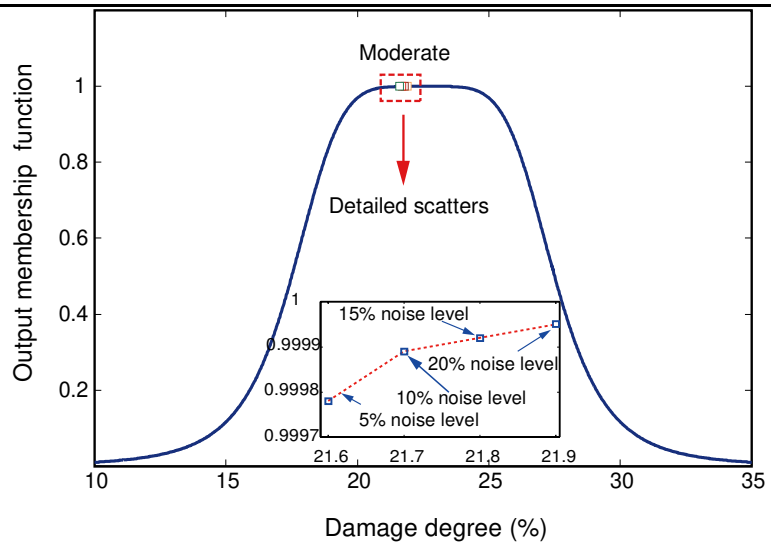

Fig. 17 FLBDI results of element ④ with 22% degradation under differernt noise levels

As shown in Fig. 17, the results of the identification of the degree of damage are 21.9%, 21.8%, 21.7% and 21.6% under the noise levels of 5%, 10%, 15% and 20%. The outputs can all be classified as 'Moderate', which corresponds to the actual degree of damage. As a result, the FLBDI method has excellent character of anti-noise characteristics, which can accurately identify the degree of damage to tunnels under a noise level of 20%.

The selection of uncertain noise level will affect the identification results, and the identification accuracy is more than 97% under the conditions of 20% noise level. The above results show that the FLBDI methods have high accuracy and good anti-noise performance. Therefore, this method will be considered to tunnel model experiments to study the damage degree identification of tunnel lining degradation in the future.

5 Conclusions

This paper proposes a new damage identification method for identifying the degree of damage in operational shield tunnels, including detecting, locating and characterizing of structural damage. Modally derived parameters and MSEDI are used to identify the location of damage and identify Level II damage. FLBDI is subsequently implemented to identify the degree of the damage and identify Level III damage. The following four conclusions are drawn:

(1) The tunnel structures modeled are approximations of circular foundation elastic beams and the modal parameters of damaged tunnel structures can be derived based on perturbation theory analysis.

The first 5^{th} modal frequency is less than 25 Hz. The maximum frequency change rate is 1.12% when the damage degree is 10%. The maximum frequency change rate is 1.99% when the damage degree is 20%. The maximum frequency change rate is 2.63% when the damage degree is 30%.

(2) For scenarios of both different damage elements and scenarios of different degrees of damage, modally derived parameters and MSEDI can properly and accurate locate the damage.

(3) Based on fuzzy logic, FLBDI can identify the degrees of damage in degraded tunnels with very high accuracy, even at noise levels reaching 20%.

(4) FLBDI also can identify the damage degrees of tunnel in degraded tunnels proficiently, considering

the incomplete information, with the accuracy of 99% and 20% noise level with the accuracy of 97%.

Acknowledgements

This work was supported by Natural Science Foundation of Jiangxi Province (20202BABL214041; 20192BAB206032) and Science and technology project of Jiangxi Provincial Transportation Department (2020Z0003; 2020X0013).

References

Anders R (1993). Vibrational based inspection of civil engineering structures. Aalborg University, Denmark.

Atluri SN (1986). Computational methods in the mechanics of fracture. Citeseer.

Beena P, Ganguli R (2011). Structural damage detection using fuzzy cognitive maps and Hebbian learning. *Applied Soft Computing*. 11: 1014-1020, DOI: 10.1016/j.asoc.2010.01.023

Bennett PJ, Soga K, Wassell I, Fidler P, Abe K, Kobayashi Y and Vanicek M (2010). Wireless sensor networks for underground railway applications: case studies in Prague and London. *Smart Structures and Systems*. 6: 619-639, DOI: 10.12989/sss.2010.6.5_6.619

Castaldo P, Calvello M and Palazzo B (2013). Probabilistic analysis of excavation-induced damages to existing structures. *Computers and Geotechnics*. 53: 17–30, DOI:10.1016/j.compgeo.2013.04.008

Castaldo P, Jalayer F and Palazzo B (2018). Probabilistic assessment of groundwater leakage in diaphragm wall joints for deep excavations. *Tunnelling and Underground Space Technology*. 71: 531–543, DOI: 10.1016/j.tust.2017.10.007

Chandrashekhar M and Ganguli R (2009). Damage assessment of structures with uncertainty by using mode-shape curvatures and fuzzy logic. *Journal of Sound and Vibration*.326: 939-957, DOI: 10.1016/j.jsv.2009.05.030

Chandrashekhar M and Ganguli R (2009). Uncertainty handling in structural damage detection using fuzzy logic and probabilistic simulation. *Mechanical Systems and Signal Processing*. 23: 384-404, DOI: 10.1016/j.ymssp.2008.03.013

Chen JC and Garba JA (1998). On-orbit damage assessment for large space structures. *AIAA journal*. 26:

1098-1126, DOI: 10.2514/3.10019

Chen S (2007). Matrix perturbation theory in structural dynamic design. Science Press, Beijing.

Doebling SW, Farrar CR and Prime MB (1998). A summary review of vibration-based damage identification methods. *Shock and vibration digest.* 30: 91-105, DOI: 10.1177/058310249803000201

Doebling SW, Farrar CR, Prime MB and Shevitz DW (1996). Damage identification and health monitoring of structural and mechanical systems from changes in their vibration characteristics: A literature review. *Shock and Vibration Digest.* 30: 2043-2049, DOI: 10.2172/249299

Farrar CR and Worden K (2007). An introduction to structural health monitoring. *Philosophical Transactions of the Royal Society A.* 365 (1851): 303-315, DOI: 10.1098/rsta.2006.1928

Feng L, Yi X, Zhu D and Xie XY (2015). Damage detection of metro tunnel structure through transmissibility function and cross correlation analysis using local excitation and measurement. *Mechanical Systems and Signal Process*ing. 60: 59-74, DOI: 10.1016/j.ymssp.2015.02.007

Fu JY, Xie J and Wang S (2019). Cracking performance of an operational tunnel lining due to local construction defects. *International Journal of Geomechanics.* 19(4): 1-13, DOI: 10.1061/(ASCE)GM.1943-5622.0001371

Ganguli R (2001). A fuzzy logic system for ground based structural health monitoring of a helicopter rotor using modal data. *Journal of Intelligent Material Systems and Structures.* 12: 397-407, DOI:

Gudmundson P (1983). The dynamic behavior of slender structures with cross-sectional cracks. *Journal of the Mechanics and Physics of Solids.* 31: 329-345, DOI: 10.1106/104538902022598

Haisty B and Springer W (1998). A general beam element for use in damage assessment of complex structures. *Journal of vibration, acoustics, stress, and reliability in design.* 110: 389-394, DOI: 10.1115/1.3269531

Hajrya R and Mechbal N (2013). Principal component analysis and perturbation theory–based robust damage detection of multifunctional aircraft structure. *Structural Health Monitoring.* 12: 263-277, DOI: 10.1177/1475921713481015

Hu MH, Tu ST, Xuan FZ, Xia CM and Shao HH (2012). Strain energy numerical technique for structural damage detection. Applied Mathematics and Computation. 219: 2424-2431, DOI: http://dx.doi.org/10.1016/j.amc.2012.08.078

Kosko B (1997). Fuzzy engineering. Los Angeles: Prentice-Hall, Inc.

Krawczuk M (2002). Application of spectral beam finite element with a crack and iterative search

technique for damage detection. *Finite Elements in Analysis and Design*.38: 537-548, DOI: 10.1016/S0168-874X(01)00084-1

Li N, Yang QW and Liang CF (2013). Structural Damage Monitoring Using the Eigenvector Perturbation Method. *Advanced Materials Research.* 1996-1999, DOI: 10.4028/www.scientific.net/AMR.838-841.1996

Liang RZ, Xia TD, Huang MS and Lin CH (2017). Simplified analytical method for evaluating the effects of adjacent excavation on shield tunnel considering the shearing effect. *Computers and Geotechnics*. 81:167-187, DOI: 10.1016/j.compgeo.2016.08.017

Luo H and Hanagud S (1997). An integral equation for changes in the structural dynamics characteristics of damaged structures. *International Journal of Solids and Structures*. 34: 4557-4579, DOI: 10.1016/S0020-7683(97)00038-3

Ostachowicz W and Krawczuk M (1991). Analysis of the effect of cracks on the natural frequencies of a cantilever beam. *Journal of sound and vibration*. 150: 191-201, DOI: 10.1016/0022-460X(91)90615-Q

Pawar PM and Ganguli R (2007). Genetic fuzzy system for online structural health monitoring of composite helicopter rotor blades. *Mechanical Systems and Signal Processing*. 21: 2212-2236, DOI: 10.1016/j.ymssp.2006.09.006

Reda TMM and Lucero J (2005). Damage identification for structural health monitoring using fuzzy pattern recognition. *Engineering Structures*. 27: 1774-1783, DOI: 10.1016/j.engstruct.2005.04.018

Rytter A (1993). Vibrational based inspection of civil engineering structures. Aalborg University.

Salawu SO (1997). Detection of structural damage through changes in frequency. *Engineering structures.* 19: 718-723, DOI: 10.1016/s0141-0296(96)00149-6

Seyedpoor S (2012). A two stage method for structural damage detection using a modal strain energy based index and particle swarm optimization. *International Journal of Non-Linear Mechanics*. 47: 1-8, DOI: 10.1016/j.ijnonlinmec.2011.07.011

Srinivas V, Ramanjaneyulu K and Jeyasehar CA (2010). Multistage approach for structural damage identification using modal strain energy and evolutionary optimization techniques. *Structural Health Monitoring*. 9: 5120-5131, DOI: 10.1177/1475921710373291

Stajano F, Hoult N, Wassell I, Bennett P, Middleton C and Soga K (2010) Smart bridges, smart tunnels: Transforming wireless sensor networks from research prototypes into robust engineering infrastructure.

Ad Hoc Networks. 8: 872-888, DOI: 10.106/j.adhoc.2010.04.002

Stepanova L and Lgonin S (2014). Perturbation method for solving the nonlinear eigenvalue problem arising from fatigue crack growth problem in a damaged medium. *Applied Mathematical Modelling*. 38: 3436-3455, DOI: 10.1016/j.apm.2013.11.057

Wahyu L (2001). Damage of Composite Structures: Detection Technique Dynamic Response and Residual Strength. Georgia Institute of Technology, Atlanta, Georgia.

Wan L, Xie XY, Wang LJ , Li P and Yin H (2021). Cavity location method for operational metro tunnels based on perturbation theory. *KSCE Journal of Civil Engineering*. 25(6): 2300-2313.

Xu H, Cheng L, Su Z and Guyader JL (2013). Damage visualization based on local dynamic perturbation: Theory and application to characterization of multi-damage in a plane structure. *Journal of Sound and Vibration.* 332: 3438-3462, DOI: 10.1016/j.jsv.2013.01.033

Xu ZD and Wu KY (2012). Damage detection for space truss structures based on strain mode under ambient excitation. *Journal of Engineering Mechanics*. 138: 1215-1223, DOI: 10.1061/(ASCE)EM.1943-7889.0000426

Yu HT and Yuan Y (2014). Analytical solution for an infinite Euler-Bernoulli beam on a viscoelastic foundation subjected to arbitrary dynamic loads. *Journal of Engineering Mechanics.* 140(3): 542-551, DOI: 10.1061/(ASCE)EM.1943-7889.0000674

Zhang J, Chen J and Wang J (2013). Prediction of tunnel displacement induced by adjacent excavation in soft soil. *Tunnelling and Underground Space Technology.* 36(36): 24-33, DOI: 10.1016/j.tust.2013.01.011

Zadeh LA (1996). Fuzzy logic—computing with words. *IEEE Transactions on Fuzzy Systems.* 4: 103-111, DOI: 10.1109/91.493904

Zhao Z and Chen C (2002). A fuzzy system for concrete bridge damage diagnosis. *Computers and Structures.* 80: 629-641, DOI: 10.1016/S0045-7949(02)00031-7

Zhang Z, Huang M and Wang W (2013). Evaluation of deformation response for adjacent tunnels due to soil unloading in excavation engineering. *Tunnelling and underground space technology*. 38: 244-253, DOI: 10.1016/j.tust.2013.07.002

Zhang Z, Huang M and Wang W (2015). A simplified analysis for deformation behavior of buried pipelines considering disturbance effects of underground excavation in soft clays. *Arabian Journal of Geosciences*. 8(10): 1-15, DOI: 10.1007/s12517-014-1773-4